PERFORMANCE OF A 40-MM COMBUSTION-HEATED LIGHT GAS GUN LAUNCHER

By

M. E. Lord

VKF, ARO, Inc.

October 1960

ARO Project No. 386601

Contract No. AF 40(600)-800 S/A 11(60-110)

AF - AEDC
Arnold AF Stn Tenn

ABSTRACT

Calculation methods and experimental results are presented for the performance of a 40-mm light gas model launcher using a mixture of helium, hydrogen, and oxygen. The effect of charging pressure on peak pressure in the chamber is given and compared to closed chamber combustion. Heat losses from the chamber were measured during cooling in the closed chamber firings. The effects of incomplete combustion were estimated. Performance of the launcher is summarized as muzzle velocity as a function of maximum chamber pressure for various projectile weights. The velocity of a 40-gram (a cylindrical slug of minimum practical weight) projectile would be 14,000 ft/sec at the maximum chamber design pressure of 60,000 psi.

CONTENTS

TABLE

ILLUSTRATIONS

NOMENCLATURE

A	Area
a	Acoustic velocity
c_v	Specific heat at constant volume
c_p	Specific heat at constant pressure
ΔH	Heat of combustion
M	Molecular weight or gm/mole of mixture
m	Mass fraction
m_p	Mass of projectile
P	Pressure
q	Heat energy per unit mass
$\dot{q}$	Heat flow rate
R	Gas constant
S_b	Length of launch tube
T	Temperature
t	Time
u	Internal energy
u_p	Velocity of projectile (Table 1)
X	Mole fraction
ρ	Density
γ	Ratio specific heats

INTRODUCTION

A 40-mm (1.58-in. bore) light gas model launcher designed by the Naval Ordnance Laboratory is installed in the Aeroballistic Branch Pilot Range. A mixture of hydrogen, oxygen, and helium is ignited to propel the projectile. The mixture has been used for development of telemeter models, optical instrumentation, and as the first stage of a two-stage 20-mm model launcher. Velocities up to 13,000 ft/sec have been obtained using a solid magnesium cylindrical projectile; however, performance charts giving the relationships between muzzle velocity, projectile weight, and completeness of combustion had not been prepared to show the limitations and the possibilities for extending the launcher performance.

The present investigation was started to study the thermodynamics of the propellant, heat losses from the combustion chamber, effect of incomplete combustion resulting from excessive charges for the diaphragm pressure limit, and launching velocity obtainable.

DISCUSSION

DESCRIPTION OF LAUNCHER DESIGN AND INSTRUMENTATION

The 40-mm H_2 -O_2 -He light gas gun launcher (Fig. 1) has a chamber 40-inches long and 2.75 inches in diameter, a diaphragm to rupture a predetermined pressure, and a smooth launch tube 26-ft long with a 1.58-inch inside diameter. A combustible mixture of hydrogen and oxygen heats helium to provide a low molecular weight propellant gas. The chamber is charged with oxygen to the required partial pressure, and an auxiliary reservoir is charged with the helium-hydrogen mixture and permitted to mix for five minutes. The chamber is then charged from the auxiliary reservoir.

The geometry of the gun range and light gas combustion gun is shown in Figs. 2 and 3. Right-circular cylindrical projectiles constructed from aluminum, magnesium, and ethocell have been used to date. The gun chamber is charged with a mixture in the ratio eight moles helium, three moles hydrogen, and one mole oxygen. Ignition of the gas mixture is performed by the discharge of a small capacitor bank through fuse wires as in Fig. 3. This discharge ignites the mixture at three points, producing

Manuscript released by author September 1960.

very satisfactory burning rates showing no evidence of detonation. This method of ignition has functioned exceptionally well with no misfires to date.

The pressure in the combustion chamber is sensed by a Norwood transducer and recorded on an oscillograph trace. The response frequency of the galvanometer was 500 cps. The time at which the projectile interrupts printed break circuits is also included on the trace. The velocity was measured with electronic counters triggered from printed circuits which are broken by the projectile. A photographic method of measuring projectile velocity has been developed, and on several shots multiple photographs were taken with the Beckman and Whitley high speed framing camera Model 195 at about 700,000 frames per second. The calculated and measured velocities are tabulated in Table 1. An oscillograph trace from a typical shot is shown in Fig. 4.

THERMODYNAMICS OF PROPELLANT

Reaction Involved

The gun chamber is charged with a mixture of helium, hydrogen, and oxygen which react as follows:

$$8\,He + 3\,H_2 + O_2 \rightarrow 8\,He + 2\,H_2O + H_2$$

The heat of combustion for the process was taken from Ref. 1 as 57800 cal/g-mole $_{H2}$ (ΔH° at 25°C). The change of heat of combustion with temperature is determined after values of the specific heats for the reactants and products are known. The process is at constant volume; therefore, the heat of combustion is equal to the change in internal energy. The final temperature can be found by determining an average specific heat at constant volume for the process.

$$\Delta H = \Delta u = c_{v\,avg}\,\Delta T$$

Specific Heats

The specific heats at constant volume were solved as a function of temperature only (Refs. 2 and 6). At the temperatures encountered, the effect of pressure on specific heat at constant volume is not appreciable. Constant volume specific heats of the reactants were determined as follows:

$$c_{v_{reactants}} = c_{v_{He}}(X_{He}) + c_{v_{H_2}}(X_{H_2}) + c_{v_{O_2}}(X_{O_2})$$

The constant volume specific heat of the products was found in a similar way. A linear burning rate was assumed as evidenced from the approximately linear pressure rise (Fig. 4). The specific heat of the mixture at any time during the process was then determined from the specific heats of the reactants and products.

$$c_{v_{mix}} = m_{products}\, c_{v_{products}} + m_{reactants}\, c_{v_{reactants}}$$

or

$$c_{v_{mix}} = \left[\frac{\%\ \text{Combustion}}{100}\right] c_{v_{products}} + \left[1 - \frac{\%\ \text{Combustion}}{100}\right] c_{v_{reactants}}$$

The average specific heat can then be found as

$$c_{v_{avg}} = \frac{1}{T - 300^{\circ}K} \int_{300^{\circ}K}^{T} c_{v_{mix}}\, dT$$

Constant volume specific heats for the reactants, products, and mixture are plotted in Fig. 5 as well as the average specific heat of the mixture. The specific heats at constant pressure for the reactants, products, and mixture were determined in a method similar to that used in determining constant volume specific heats. These results are plotted in Fig. 6.

Determination of Final State Point

The heat of combustion is equal to the change in internal energy for a combustion process at constant volume, or

$$\Delta H = u_{products} - u_{reactants}$$

$$\frac{d(\Delta H)}{dT} = \frac{d(u_{products})}{dT} - \frac{d(u_{reactants})}{dT}$$

$$\frac{d(\Delta H)}{dT} = c_{v_{products}} - c_{v_{reactants}}$$

$$\int_{T_1}^{T_2} d(\Delta H) = \int_{T_1}^{T_2} c_{v_{products}}\, dT - \int_{T_1}^{T_2} c_{v_{reactants}}\, dT$$

$$(\Delta H)_{T_2} - (\Delta H)_{T_1} = \int_{T_1}^{T_2} c_{v_{products}}\, dT - \int_{T_1}^{T_2} c_{v_{reactants}}\, dT$$

This expression was used to calculate the change in heat of combustion during the process. It was found that the heat of combustion changed only 1.7 percent of the value at 25°C. Therefore, the heat of combustion was assumed a constant value (ΔH = 57800 cal/g-mole$_{H_2}$ or 1650 cal/gm$_{mix}$). The final temperature of about 2700°K is obtained by integrating the $c_{v_{avg}}$ above to the point where $\int_{300}^{T} c_{v_{avg}}\, dT$ is equal to the heat of combustion, ΔH.

The molecular weight of the products is determined as

$$M_{products} = M_{He}\,(X_{He}) + M_{H_2}\,(X_{H_2}) + M_{O_2}\,(X_{O_2})$$

and the gas constant for the products is

$$R_{products} = \frac{R_o}{M_{products}} = \frac{1.986 \text{ cal/mole °K}}{6.37 \text{ gm/mole}} = 0.312 \text{ cal/gm°K}$$

The final pressure will be a function of the charge density (or pressure) for a constant final temperature. A final pressure calculation was made assuming perfect gas relations.

$$P_{final} = \rho_{charge}\, R_{products}\, T_{final}$$

The charge pressure is directly proportional to the charge density; therefore, the results of the above equation are plotted in Fig. 7 as theoretical final pressure as a function of charge pressure. The process usually was not completed because the diaphragm usually failed before a maximum pressure was reached. This would produce a decrease in temperature and in acoustic velocity. The percent combustion was determined as the percent of the actual maximum pressure reached at the time the diaphragm failed. The percent of combustion will determine the temperature of the mixture, and hence, acoustic velocity. The temperature also determines the specific heat values and the value of γ. The acoustic velocity and the value of γ as determined in terms of the percent combustion are plotted in Fig. 8. These results will be used later for calculating projectile velocity.

A few contained, or closed chamber, shots were made to determine results of 100-percent combustion. During the contained shots the diaphragm was replaced by a solid retainer, thus containing the pressure in the chamber. The actual maximum pressures attained during these 100-percent combustion shots are compared with the theoretical pressures in Fig. 7. A correction for heat loss during combustion (see the next page) was made, and the actual 100-percent combustion curve was faired through the corrected experimental points. A pressure decay was also obtained during the contained shots which produced a method for calculating heat loss rates from the chamber.

Heat Transfer

During the contained gun shots a record of the pressure decay was taken. A heat flux can be calculated as follows:

$$\dot{q} = \frac{\partial q}{\partial t} = \frac{\partial q}{\partial T} \cdot \frac{\partial T}{\partial t}$$

but $$\left(\frac{\partial q}{\partial T}\right)_v = c_v$$

and $$\frac{\partial T}{\partial t} = \frac{1}{R\rho} \frac{\partial P}{\partial t}$$ where density is constant and R is gas constant for the products

therefore, $$\dot{q} = c_v \frac{1}{R\rho} \frac{\partial P}{\partial t}$$

The results of the contained shots are shown in Fig. 9 as a plot of heat flux vs temperature for a family of charge pressures. An estimate of the heat loss during the combustion process was made by assuming the heat rate for the combustion process equal the heat rate during the cooling process. This assumption was made because of the lack of information on thermal conductivity of non-equilibrium gas mixtures. Although the conductivity between the non-equilibrium and equilibrium mixtures may vary considerably, it was hoped that some relation between the pressure loss and heat transfer could be established. The measured peak pressures and the adiabatic pressure, pressure corrected for heat losses, are plotted in Fig. 7.

PERFORMANCE OF LAUNCHER

Estimated Gun Performance

To calculate the projectile velocity the following interior ballistic equation (Ref. 3) was used:

$$\frac{A\rho S_b}{m_p} = \frac{2\gamma}{\gamma - 1}\left\{\frac{2}{\gamma + 1}\left[1 - \frac{\gamma - 1}{2}\frac{u_p}{a_c}\right]^{-\frac{\gamma+1}{\gamma-1}} - \left[1 - \frac{\gamma - 1}{2}\frac{u_p}{a_c}\right]^{-\frac{2}{\gamma-1}} + \frac{\gamma - 1}{\gamma + 1}\right\}$$

The results of this equation assuming actual 100-percent combustion (γ = 1.39 and a_c = 7150 ft/sec) are shown in Fig. 16. The percent combustion was determined from the ratio of the pressure to actual 100-percent combustion pressure for the evaluation of the data. The value of γ and acoustic velocity were then obtained from Fig. 8. The projectile velocity was therefore determined in terms of the state point at the time the diaphragm failed. These velocities (calculated) are compared in Table 1 with the velocities measured with the printed circuits and Beckman and Whitley camera. The measured muzzle

velocity was determined by extrapolation of the down range velocities. The calculated velocity assumed no energy added after the diaphragm failed, but actually the gases continue to burn and influence the projectile up to the time the projectile leaves the muzzle. The extent of this additional energy effect will depend on the time the projectile is in the barrel and also on the rate at which combustion is taking place. For a fixed burning rate, the slower the projectile acceleration, the more it will be affected by additional burning; likewise, for a fixed projectile acceleration, the faster the burning rate, the more energy will be added to the propellant gases.

An estimate of the time the projectile was in the barrel was made from the muzzle velocity. It was assumed that for one-third of this time, the gases continued to burn contained. The pressure trace was extrapolated one-third of the time the projectile was in the barrel, and an effective chamber pressure (P_{eff}) was determined. A typical pressure trace for a low percent combustion shot is shown in Fig. 4 with an extrapolation to an effective pressure. This procedure was carried out for each shot, and an effective velocity was calculated from this effective pressure. These results are tabulated in Table 1 (Effective Calculated Velocity). The measured velocities are from 0.90 to 1.10 of effective calculated velocities, averaging about 1.5 percent over the effective calculated velocities.

Chambrage

The internal ballistic equation used in calculating projectile velocity assumes unrestricted flow of the propellant gases from the breech to the barrel. However, if there is a reduction in chamber to bore diameter, the flow will become choked, thus producing an additional pressure rise in the propellant gases in the bore. This pressure rise is determined by the amount of chambrage, that is, ratio of bore to chamber diameter. The effect of chambrage is discussed fully in Ref. 5, and experimental results are presented in Ref. 4. From the experimental results of Ref. 4 the effect of chambrage on the combustion gun performance was determined. These results show a velocity increase for the combustion gun geometry of 10 to 11 percent over a gun of unit chambrage. Correcting for this effect yields an average effective, calculated velocity about 8-percent greater than that obtained experimentally. The neglected effects of bore friction, non-ideal propellant expansion, and heat losses contribute to the lower experimental velocity. These two effects appear to have approximately the same magnitude in the present results, thus accounting for the close agreement between the measured and effective calculated velocities.

Reliability of the pressure gages used in charging the gun was approximately ±500 psi. This much deviation in charge conditions could affect the final pressure by ±3000 psi. At 20,000-psi chamber pressure the deviation would have a ±8-percent effect on velocity; whereas, at 50,000 psi the effect on velocity would be ±3 percent.

CONCLUDING REMARKS

The results of the contained shots indicate that very little pressure is lost due to heat transfer during the combustion process. The maximum loss in pressure due to heat transfer is 4.9 percent. The greatest loss of energy is associated with incomplete combustion caused by the diaphragm failing at too low a pressure. The diaphragm should fail just as the pressure reaches a peak for optimum performance. From results of the low percent combustion shots, it is evident that the projectile does experience the addition of energy after failure of the diaphragm. Although the method of calculating the effect of the continued burning is crude, it does provide a method of determining the trend of the effect of low percent combustion.

The development of a diaphragm system to contain the chamber charge until combustion is complete would insure consistent launcher performance.

The 40-mm combustion gun has been of great assistance in the development of photographic techniques and of telemetering. It has provided a means of successfully launching projectiles capable of carrying telemetering packages to velocities in the ranges of 6000 to 12,000 ft/sec.

One obvious limitation of the combustion gun is its sonic speed. Assuming 100-percent combustion, the sonic speed is a fixed value; therefore, for a fixed projectile mass the only way of gaining higher projectile velocity is by increasing the chamber pressure. As can be seen from Fig. 10, the rate of increase of velocity with chamber pressure decreases with increasing chamber pressure. By increasing the chamber pressure from 50,000 to 100,000 psi (a 100-percent pressure increase) for a 60-gm projectile the velocity increases from 12,600 ft/sec to 14,200 ft/sec, thus realizing a velocity increase of 13 percent. A temperature increase from 2700°K to 3450°K would produce an equal increase in velocity.

REFERENCES

1. Obert, E. F. Thermodynamics. McGraw-Hill Book Company, New York, 1948.

2. Ellenwood, F. O., Kulik, N. and Gay, R. N. "The Specific Heats of Certain Gases Over Wide Ranges of Pressures and Temperatures." Cornell University Bulletin No. 30, October 1942.

3. Charters, A. C., Denardo, P., and Rossow, V. J. "Development of a Piston-Compressor Type Light-Gas Gun for the Launching of Free-Flight Models at High Velocity." NACA TN 4143, November 1957.

4. Seigel, A. E. and Dawson, V. C. D. "Results of Chambrage Experiments on Guns with Effectively Infinite Length Chambers." NAVORD Report 3636, April 1954.

5. Seigel, A. E. "The Influence of Chamber Diameter Size on the Muzzle Velocity of a Gun with Effectively an Infinite Length Chamber." NAVORD Report 3635.

6. Leduc, A. "The Heat Capacities of Gases and Vapors." National Research Council, International Critical Tables, Numerical Data, Physics, Chemistry, and Technology, Vol. V, McGraw-Hill Book Company, 1929, pp. 79-84.

TABLE 1

COMPARISON OF CALCULATED AND MEASURED VELOCITIES

Round No.	P_{chg} psi	P_{final} psi	m_p gm	Percent** Combustion	Measured Velocity fps	Calculated Velocity fps	Effective Pressure psi	Effective Calculated Velocity fps	$\frac{u_{P_{meas.}}}{u_{P_{eff. cal.}}}$
25	9,000	35,300	70.5	64	10,500	9,430	37,000	9,700	1.08
26	9,000	33,500	150.0	61	8,500	7,700	36,300	8,000	1.06
31	8,700	48,000	70.9	91	11,300	11,500	50,500	11,800	0.96
32	8,700	40,000	100.0	75	9,900	9,500	43,300	9,900	1.00
36	9,500	51,000	200.0	90	9,300	9,050	52,000	9,150	1.02
40	9,500	43,000	39.8	76	12,500	11,800	45,500	12,100	1.03
44*	9,000	33,000	175.0	60	7,900	7,300	33,500	7,350	1.07
46*	7,000	24,600	158.0	56	8,300	6,950	32,000	7,950	1.04
63	6,500	27,500	98.5	66	9,600	8,400	29,700	8,750	1.10
65*	4,500	30,000	168.0	97	7,500	8,300	30,500	8,350	0.90
67*	4,500	19,500	98.2	63	8,060	7,550	21,000	7,850	1.03
68	5,500	23,000	98.7	64	8,000	7,850	25,000	8,200	0.98
70	7,000	25,500	45.6	58	10,300	9,350	26,800	9,550	1.08
75	7,500	32,300	45.4	69	11,300	10,500	37,300	11,300	1.00
77	7,500	33,000	49.0	70	10,600	10,300	38,000	11,050	0.93
79*	3,500	19,700	95.7	74	8,100	8,150	21,500	8,500	0.95

*Velocities checked by Beckman and Whitley camera

**Percent of actual complete combustion (Fig. 7)

Fig. 1 Combustion Gun and Range

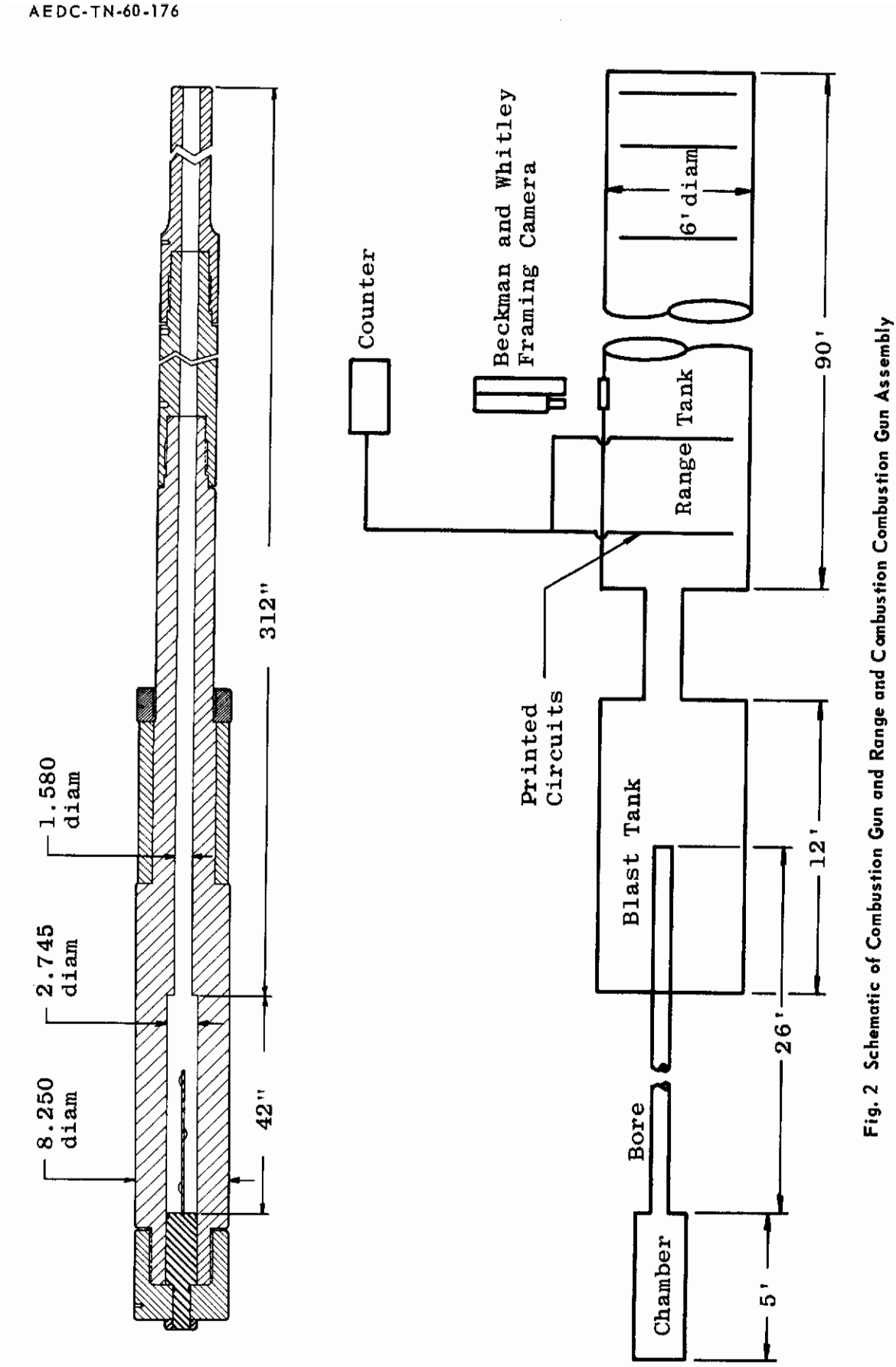

Fig. 2 Schematic of Combustion Gun and Range and Combustion Combustion Gun Assembly

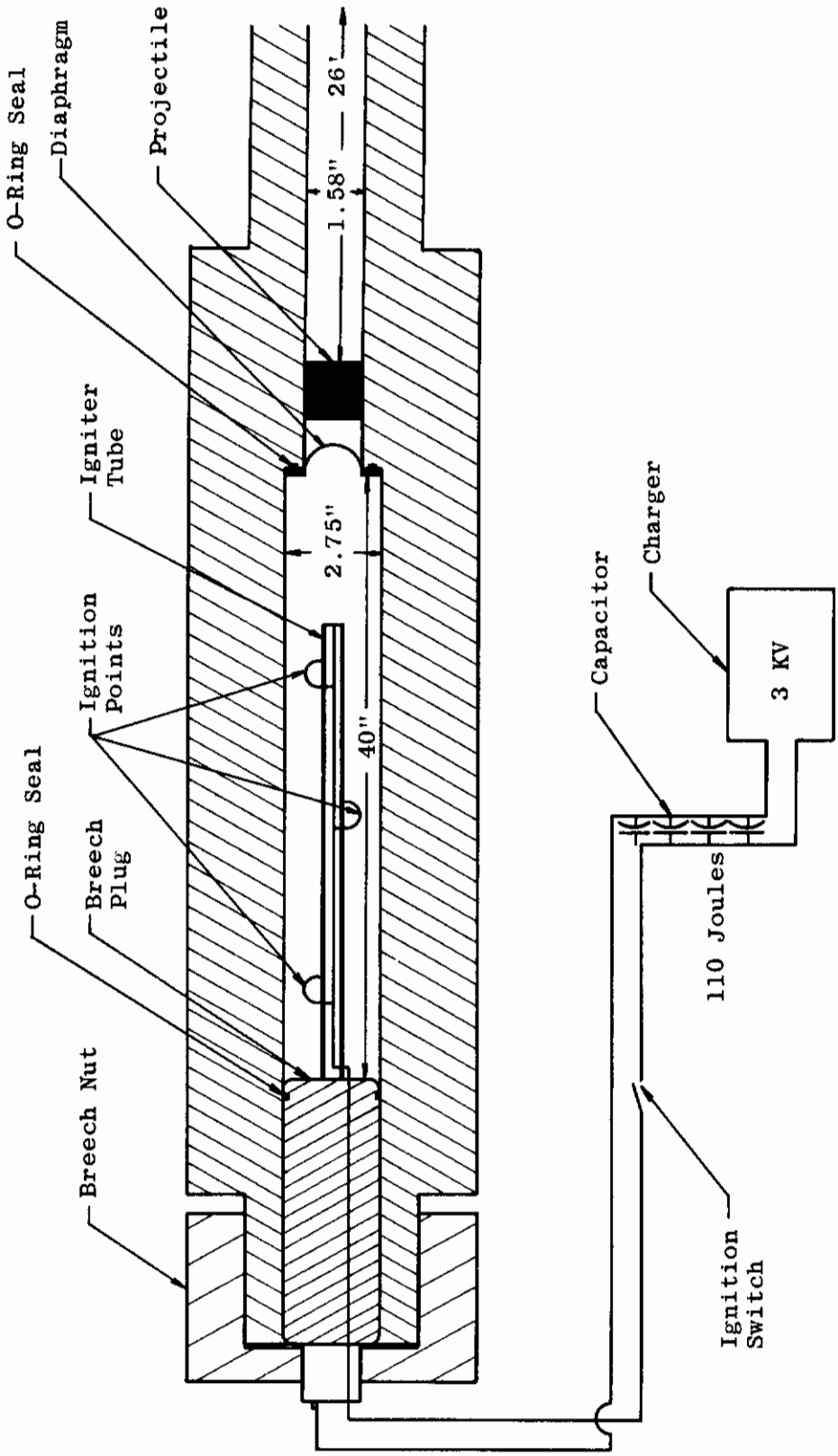

Fig. 3 Combustion Gun Chamber Assembly and Ignition Diagram

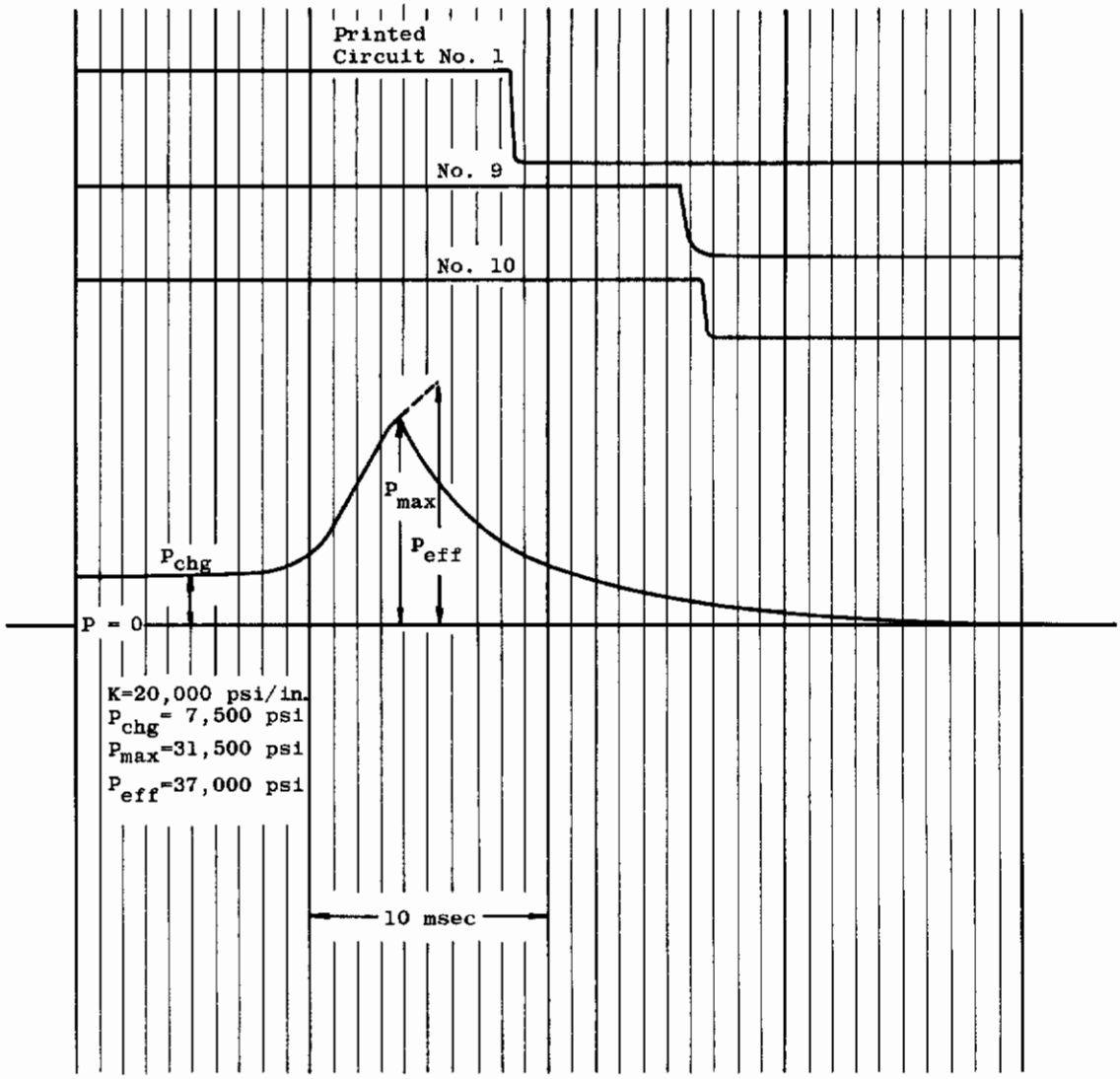

Fig. 4 Typical Oscillograph Trace

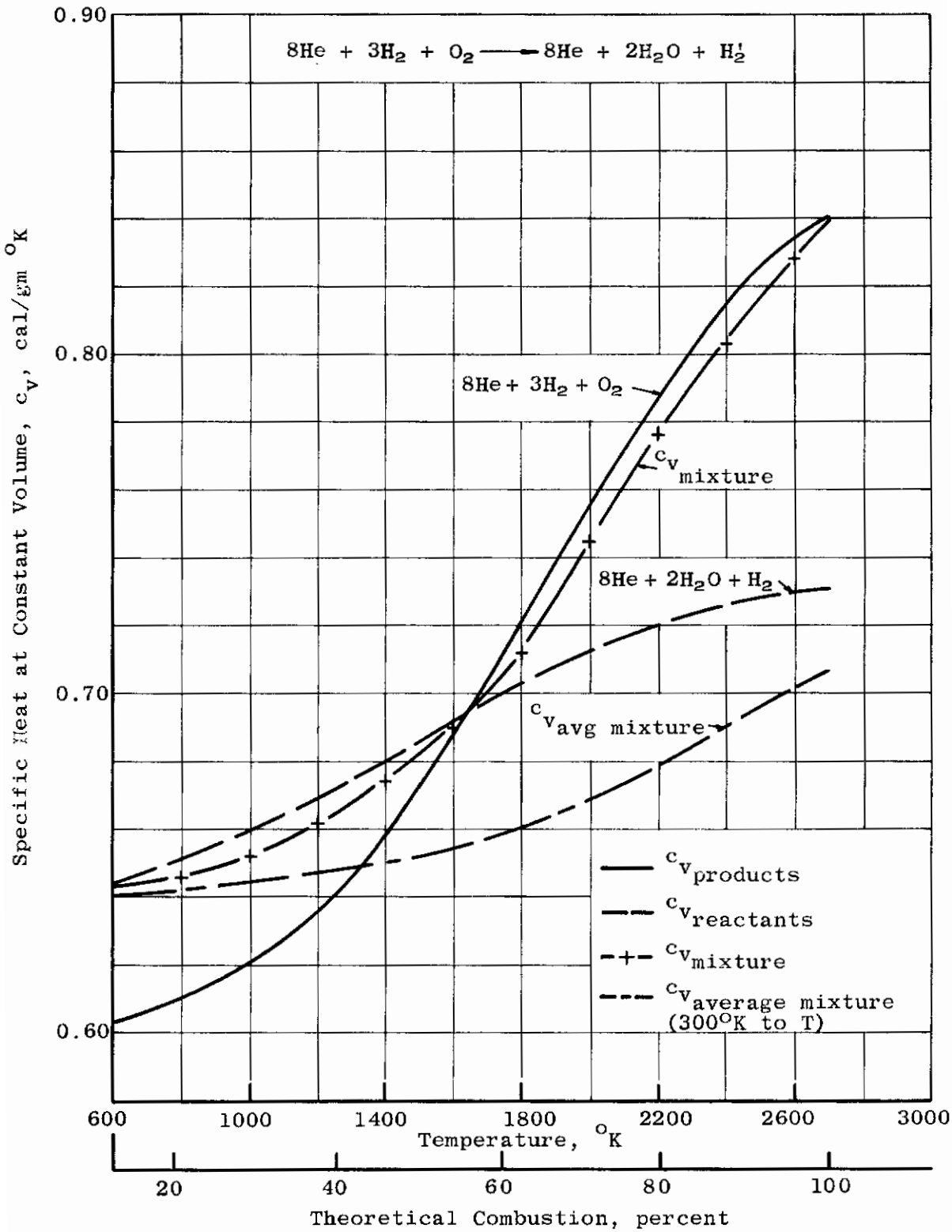

Fig. 5 Constant Volume Specific Heat vs Temperature

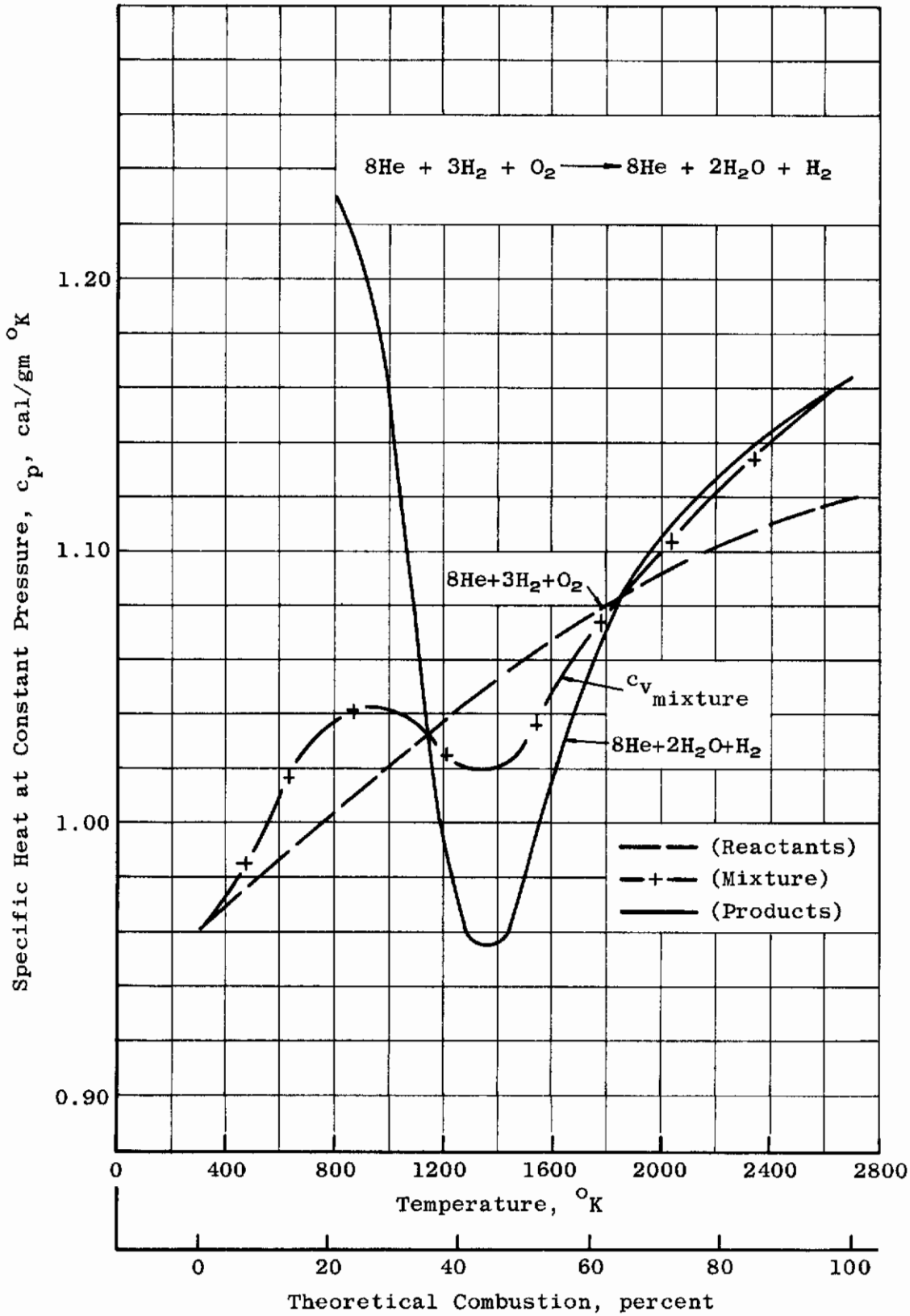

Fig. 6 Constant Pressure Specific Heat vs Temperature

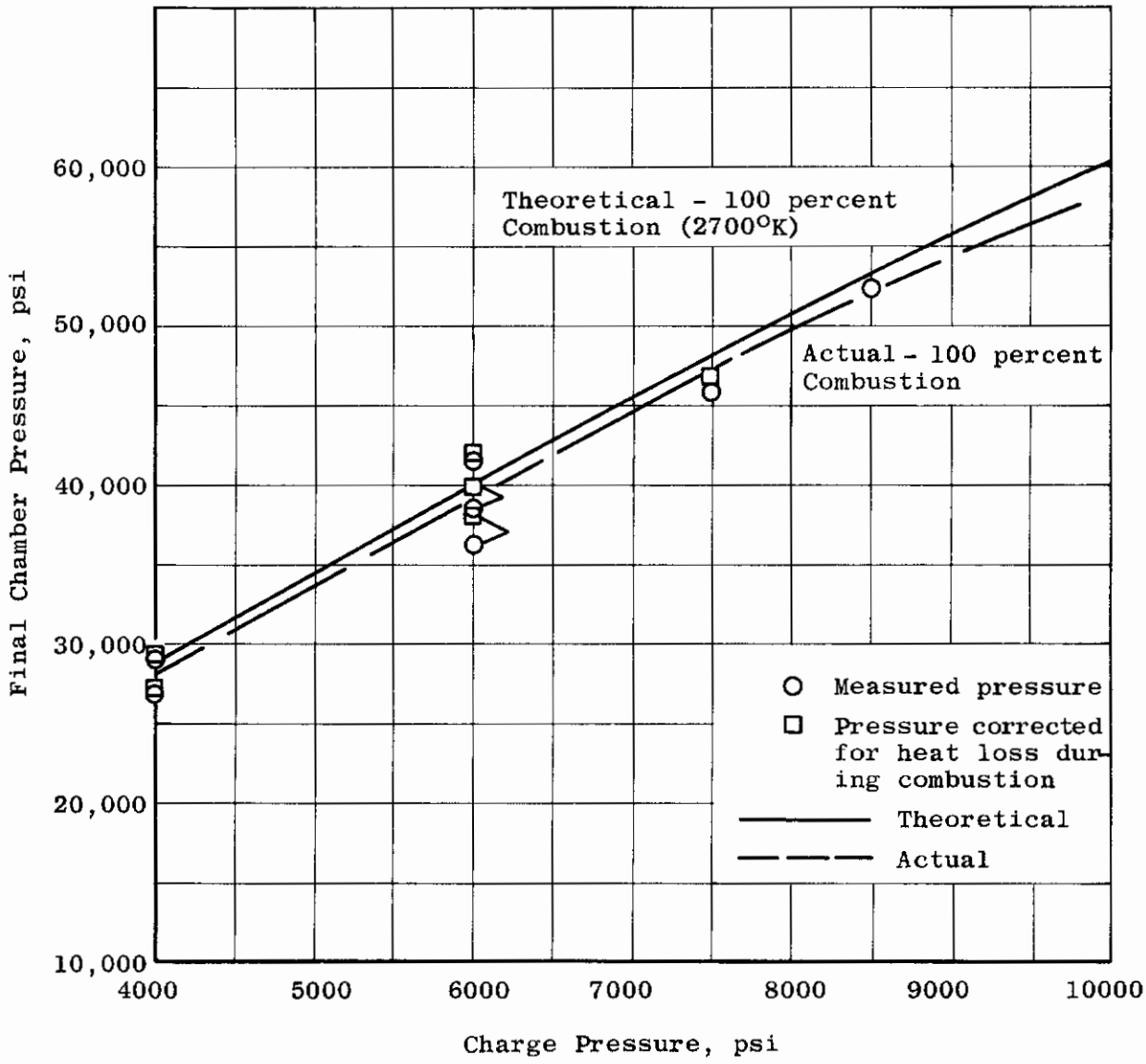

Fig. 7 Final Chamber Pressure vs Charge Pressure

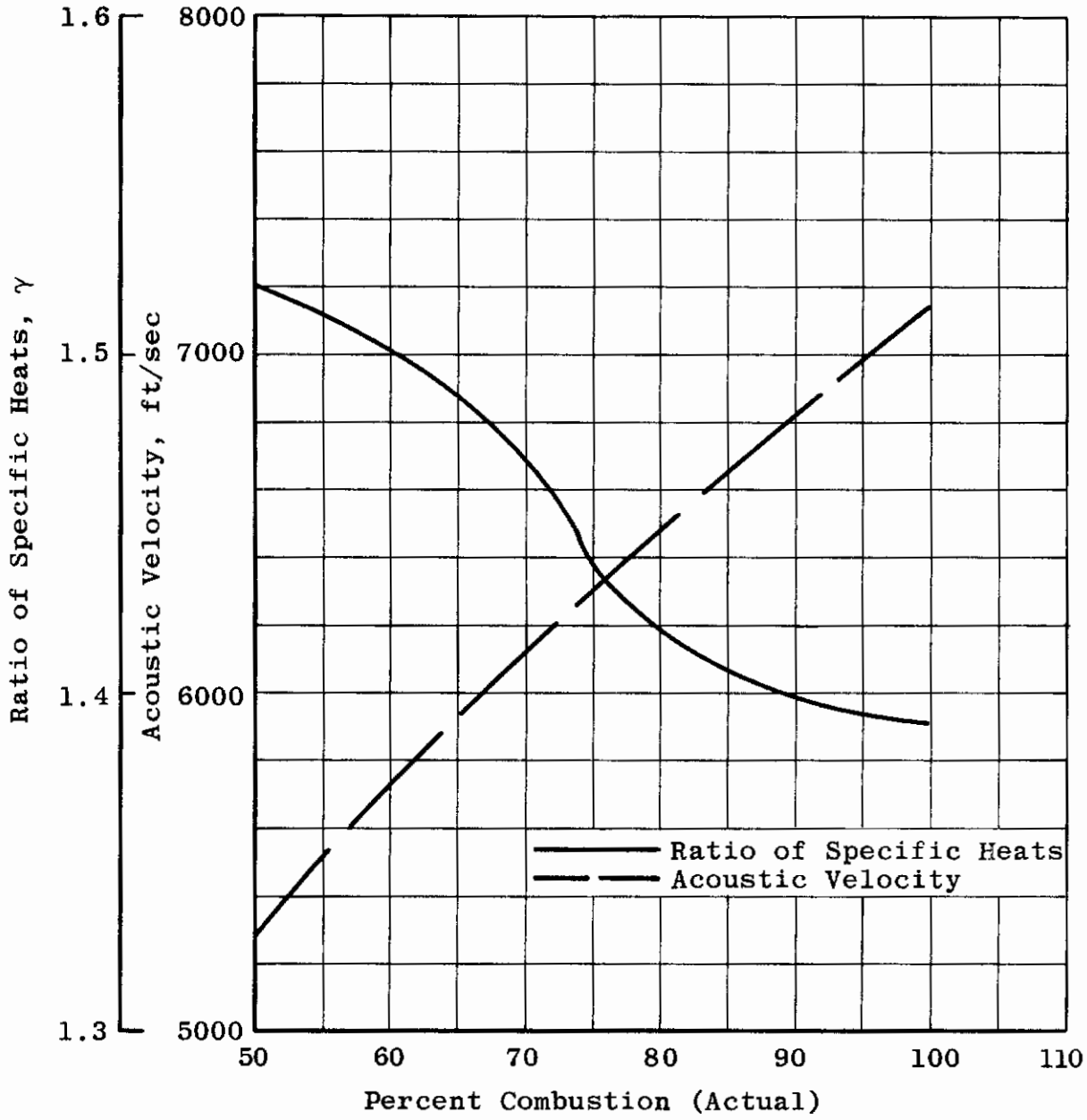

Fig. 8 Ratio of Specific Heats and Acoustic Velocity vs Percent Combustion (Actual)

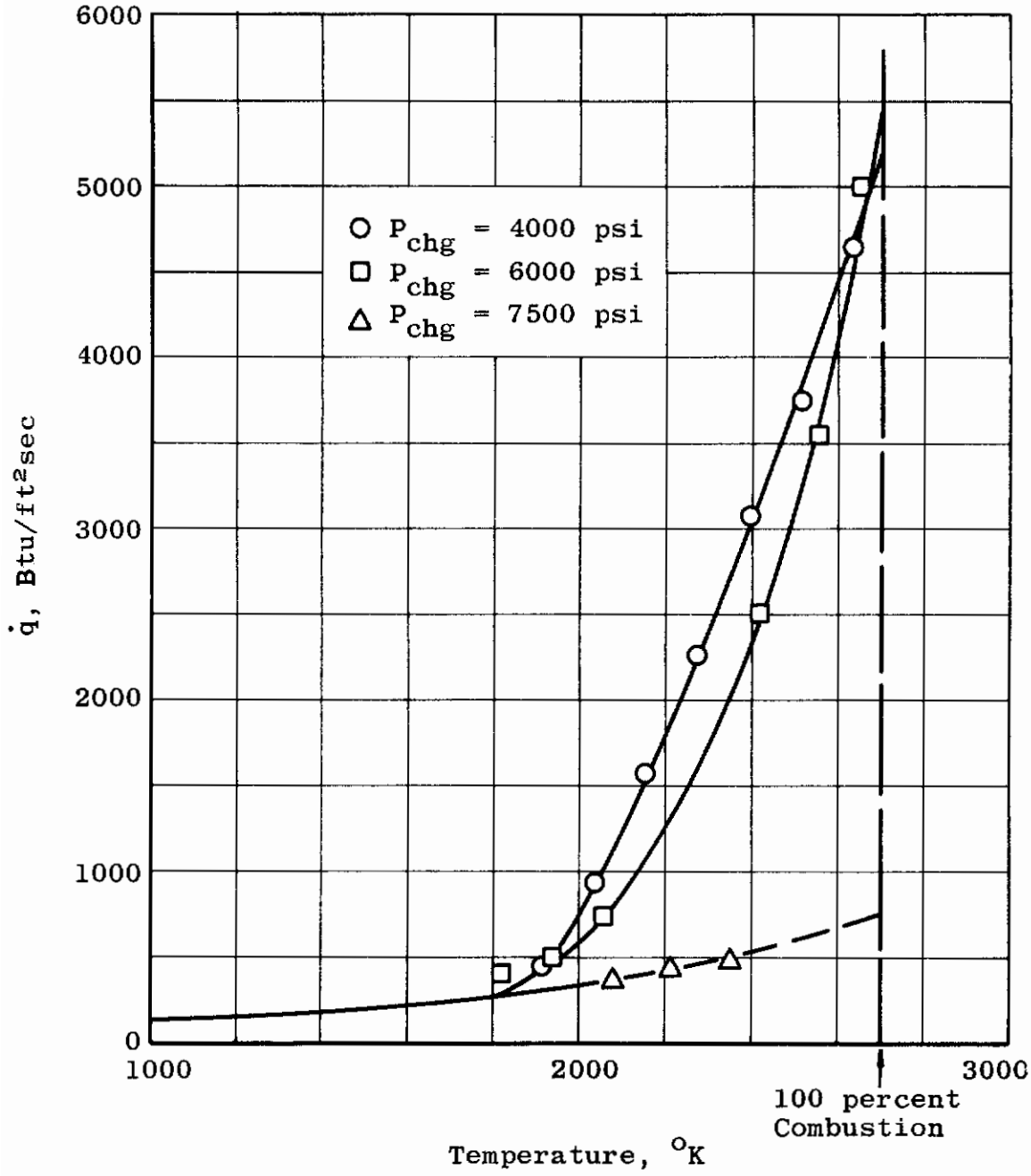

Fig. 9 Heat Transfer from Chamber

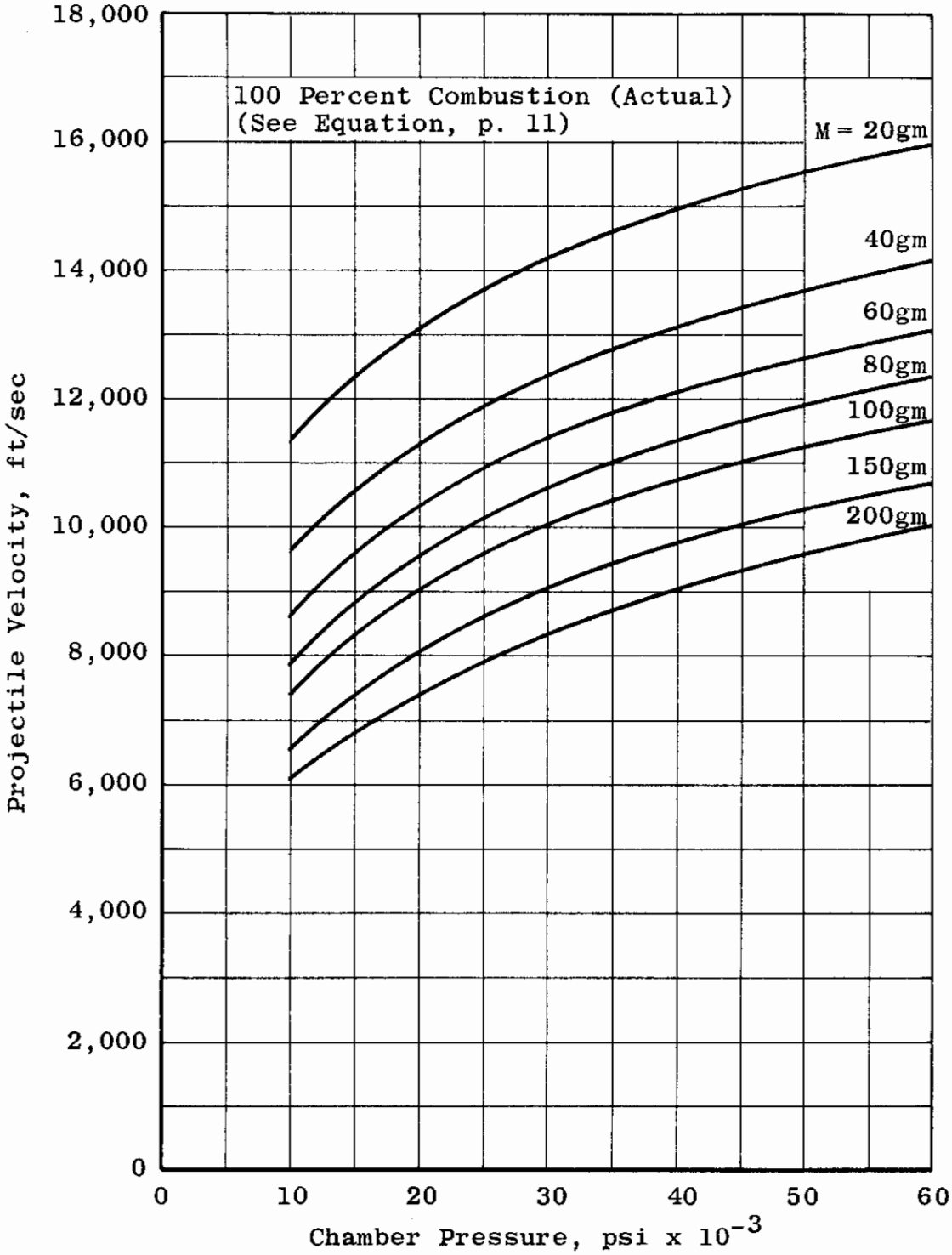

Fig. 10 Velocity Performance